LONGITUDINAL BEAM ECHO IN THE CERN SPS

O. Brüning, T. Linnecar, F. Ruggiero, W. Scandale, E. Shaposhnikova, D. Stellfeld
CERN, Geneva, Switzerland

Abstract

The presented work summarises the results of two experiments in the CERN SPS. Longitudinal echo signals can be produced in the CERN-SPS by exciting a coasting proton beam at 120 GeV/c with two short RF pulses at different harmonics of the revolution frequency, separated by a suitable time-delay. The aim of the experiments was to confirm the analytical predictions for a beam echo in the SPS and to probe the applicability of the beam echo for a measurement of the energy distribution and diffusion coefficients in the accelerator.

1 INTRODUCTION

Echo phenomena have been well known in plasma physics for many years [1]. However, the effect has only been recently introduced to accelerator physics. The first measurements of the effect were made one year ago in the 8 GeV anti-proton accumulator ring at FNAL [2]. These first results were very promising and encouraged further studies. For example, echo techniques might offer a new approach for investigating diffusion and collective effects in hadron storage rings [2]. The aim of the presented work was to measure echo signals in the CERN SPS and to investigate the applicability of the beam echo for a measurement of the energy distribution and diffusion coefficients in the accelerator.

The echo signal is an interference pattern of two consecutive short RF-pulses. A theoretical analysis of the echo effect shows that the time and the amplitude of the echo response depends on the time delay between the two RF-kicks. The basic idea of the analysis is to treat the energy gain during the two RF-kicks as small perturbations and to expand the initial distribution function in a Taylor series around the unperturbed variables [3].

Without diffusion, the equations of motion for a coasting beam can be easily solved and one can show that the beam echo appears at a time

$$t^* = \frac{h_1}{h_2 - h_1} \cdot \triangle t \tag{1}$$

after the second RF-kick, where $\triangle t$ is the time separation of the two RF-kicks. Adding diffusion to the particle dynamics and using similar approximations as in the case without diffusion, one gets for the echo response in the beam current [3][4]

$$\begin{aligned} I_{echo}(t) \;\approx\; & e\omega_0 2\epsilon_1 \cdot \{J_1(x) + \tau\epsilon_2 [J_0(x) - J_2(x)]\} \\ \times \quad & \tau \cdot \int \rho(p) \cdot \cos(p\tau)\; dp \\ \times \quad & e^{-Dk_0^2\left[h_1^2(\triangle t)^3 + (h_2 - h_1)^2 \cdot t^3\right]/3}, \end{aligned} \tag{2}$$

where D is the diffusion coefficient, $\rho(p)$ the initial energy distribution, τ the time measured relative to the centre of the echo response ($\tau = k_0(h_2 - h_1) \cdot (t - t^*)$) and t the time measured from the second RF kick. $J_n(x)$ are Bessel functions of the first kind with

$$x = 2h_1\epsilon_2\sigma_p k_0 \triangle t \tag{3}$$

and

$$k_0 = \frac{\omega_0 \eta}{\beta^2}; \qquad \eta = \frac{1}{\gamma_t^2} - \frac{1}{\gamma^2}. \tag{4}$$

ϵ_1 and ϵ_2 are the perturbation parameters in the Taylor expansion

$$\epsilon_i = \frac{\omega_0 T_i}{2\pi} \cdot \frac{eV_i}{E_0}; \qquad i = 1, 2 \tag{5}$$

where T_1 and T_2 are the kick lengths and V_1 and V_2 are the kick amplitudes of the first and second RF kick respectively. The strong cubic dependence of the damping term on time suggests the possibility of measuring even very small diffusion coefficients in a reasonably short time interval. Furthermore, Equation (2) indicates a strong influence of the actual energy distribution on the shape of the echo signal, suggesting the possibility of measuring the energy distribution in the storage ring with the echo response. For example, Fig. 1 shows the absolute value of the analytical estimate for the echo response for a Gaussian energy distribution and Fig. 2 the analytical estimate for a parabolic energy distribution [4].

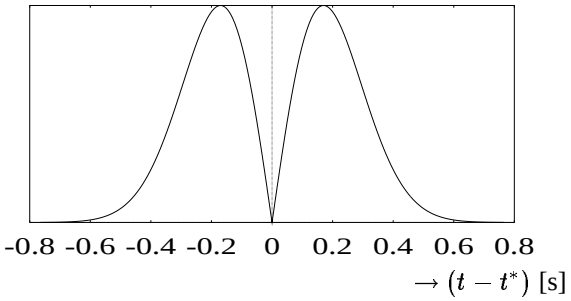

Figure 1: *The analytical estimate for the echo shape for a Gaussian energy distribution:* $\triangle t$ *= 45 ms,* $\sigma_p = 6 \cdot 10^{-4}$ *and parameters of Table 1.*

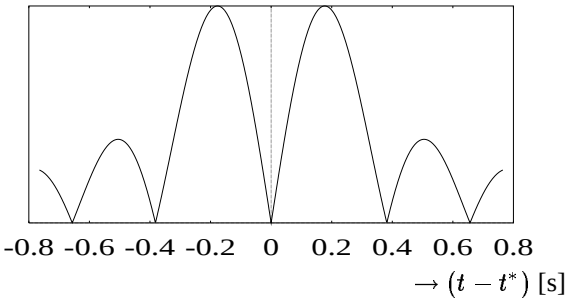

Figure 2: *The analytical estimate for the echo shape for a parabolic energy distribution:* $\triangle t = 45$ *ms and the parameters of Table 1.*

2 EXPERIMENTAL DATA

Fig. 3 shows the experimental setup for the echo measurement. All the data discussed in this section was measured

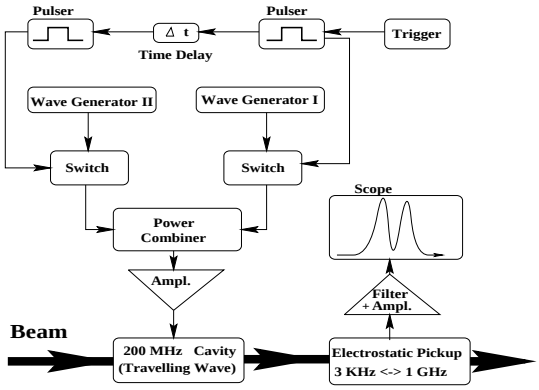

Figure 3: *Schematic setup for the Echo measurements.*

for two RF kicks with harmonic numbers $h_1 = 4600$ and $h_2 = 4620$ and a kick amplitude of 500 kV per kick. Each kick lasted for approximately 4 turns ($T_i \approx 92.221\,\mu s$). The beam intensity was approximately $1.2 \cdot 10^{12}$ particles. Table 1 lists the relevant parameters for the CERN SPS storage ring. Fig. 4 shows a longitudinal Schottky spectrum towards

f_{rev} [kHz]	η	E_0 [GeV]	f_{RF} [MHz]
43.23	$1.8 \cdot 10^{-3}$	120	200

Table 1: *Machine parameters of the SPS.*

the beginning of a new proton fill and Fig. 5 shows the corresponding echo signal for a time separation of the two RF kicks of $\triangle t = 45\ ms$. One clearly recognises the multiple peaks from a non-Gaussian energy distribution. Fig. 6 shows a longitudinal Schottky spectrum approximately 1 hour after the injection of a proton fill and Fig. 5 shows the corresponding echo signal. The time separation of the two RF kicks was again $\triangle t = 45\ ms$. In this case, the measured echo response corresponds to an approximately Gaussian energy distribution.

Both examples illustrate nicely the sensitivity of the echo

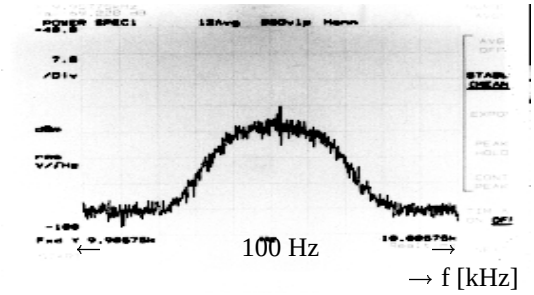

Figure 4: *The measured energy distribution in the longitudinal Schottky spectrum. The horizontal scale extends from 9.90575 kHz to 10.90575 kHz.*

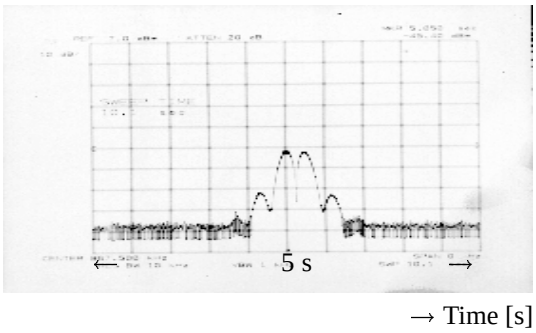

Figure 5: *The measured echo signal on a logarithmic scale. The measurement corresponds to the beam distribution in Fig. 4. One clearly recognises the multiple peaks from a non-Gaussian energy distribution.*

response on the energy distribution in the beam. In principle, the distribution function can be recovered by an inverse Fourier transform of the echo response (see Equation (2)). However, a detailed study of this potential application for beam echos is still in progress and a reconstruction of the energy distribution from the beam echo has not yet been done. The energy spread in the beam distribution is given by the time separation $\triangle_{peak}$ of the two maxima in the echo response. For example, for a Gaussian energy distribution,

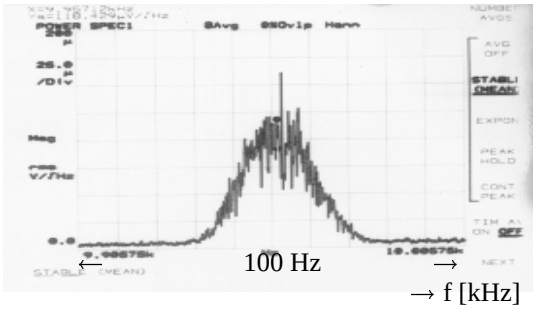

Figure 6: *The measured energy distribution in the longitudinal Schottky spectrum. The horizontal scale extends from 9.90575 kHz to 10.90575 kHz.*

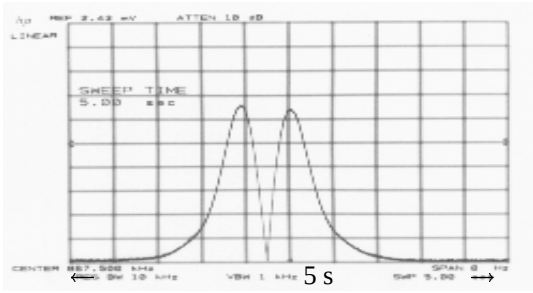

Figure 7: *The measured echo signal on a linear scale. The measurement corresponds to the beam distribution in Fig. 6. The measured echo response corresponds to an approximately Gaussian energy distribution.*

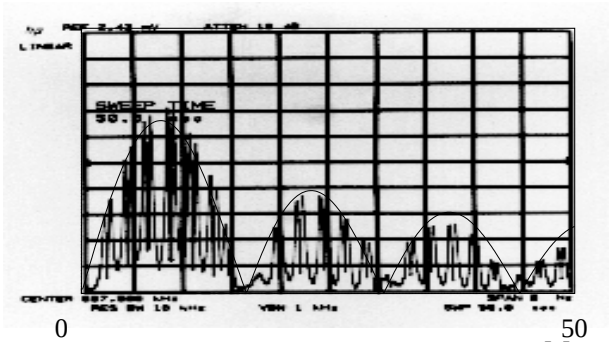

Figure 8: *The picture shows the superposition of 22 beam echos for different separation times $\triangle t$ as a function of time after the second RF kick. The time separation of the two RF kicks varies between 5 ms and 220 ms. The solid envelope shows the analytical estimate for the maximum echo response from Equation 2 with $D = 0$.*

one obtains from Equation (2)

$$\sigma_p = \frac{\beta^2}{(h_2 - h_1) \cdot \pi \cdot f_{rev} \cdot |\eta| \cdot \triangle_{peak}}. \qquad (6)$$

Using Equation (6), we get from Fig. 7 $\sigma_p = 4.1 \cdot 10^{-4}$. Measuring the energy spread directly from the longitudinal Schottky signal in Fig. 6, we get $\sigma_p = 5.2 \cdot 10^{-4}$. Both values agree rather well. However, reading the frequency spread from the Schottky signal is more cumbersome than reading the time separation of the two maxima in the echo signal.

Fig. 8 shows a series of 22 echo measurements for different time separations between the two RF kicks. The vertical axis shows the amplitude of the echo response and the horizontal axis the time measured after the second RF kick. The appearance of the echo signal is proportional to the time delay between the two RF kicks (see Equation (1)) and the beam echo appears the later in time, for a larger time separation between the two RF kicks. The time separation in Fig 8 varied between 5 ms and 220 ms and horizontal scale varies from 0 s to 50 s. The solid envelope shows the analytical estimate for the maximum echo response from Equation 2. Because the amplitude of the measured beam echo depends on the amplification and the electronics in the monitor, we had one free parameter to adjust the amplitude of the measured beam echo to the analytical prediction. In Fig.8 we used this free parameter for matching the amplitude of the first maximum in the measured data with the analytical estimate. Up to a time separation of 130 ms, or echo signals which appear within 30 s after the second RF kick, the agreement between the analytical estimate (2) and the measured echo signal is rather good. For a time separation of more than 130 ms, the measured echo response is slightly smaller than the analytical estimate. The introduction of a non-vanishing diffusion term ($D = 10^{-13} s^{-1}$) to Equation (2) results in a very good agreement between the measured envelope and the analytical estimate even for a time separation of the two RF kicks of more than 130 ms. (A small diffusion coefficient of $D = 10^{-13}$ results in a doubling of the energy spread after 10^7 s.) A detailed study of the effect of diffusion on the beam echo is still in progress. In a recent experiment in the CERN SPS storage ring an additional diffusion was generated by applying a noise signal to one of the RF cavities. The noise signal was calibrated by measuring the growth of the energy spread in the beam for different noise amplitudes with the longitudinal Schottky signal. Over a time interval of 100 s, the Schottky signal was sensitive to noise signals which correspond to $D > 10^{-9} s^{-1}$. Once the noise signal was calibrated the noise amplitude was reduced to values where we could no longer observe a growth of the energy spread in the longitudinal Schottky signal ($D < 10^{-9} s^{-1}$). The beam echo could be successfully used to measure noise amplitudes which were at least two orders of magnitude smaller ($D \approx 10^{-11} s^{-1}$).

3 CONCLUSIONS

The beam echo measurements in the CERN SPS agree well with the analytical expectations and encourage attempts to use the beam echo for measurements of beam distributions and diffusion coefficients in the beam. The measurement of intensity dependent effects might be another potential application of beam echoes. The ongoing study at the CERN SPS foresees to analyse the effect of wake fields on the beam echo in the upcoming experiments. So far, the studies in the CERN SPS were limited to longitudinal beam echos in an un-bunched beam. However, the ongoing work aims at extending the studies to bunched beams and to the transverse plain.

4 REFERENCES

[1] T.M. O' Neil and R.W. Gould, Phys. Fluids **11**, 1 (1968).

[2] L.K. Spenzouris, J.-F. Ostigy, P.L. Colestock, Phys. Rev. Letters **76**, 620 (1996).

[3] O. Brüning, CERN SL/95-83 (AP), 1995.

[4] E. Shaposhnikova, CERN SL-Note 95-125 (RF), 1995.